# MONTE-CARLO-SIMULATION IN CLOSE-RANGE PHOTOGRAMMETRY

Heidi Hastedt

Institute of Applied Photogrammetry and Geoinformatics, Oldenburg, Germany, h.hastedt@vermes.fh-oldenburg.de

**Commission V, WG V/1**

**KEY WORDS:** Accuracy, Adjustment, Calibration, Metrology, Modelling, Photogrammetry, Simulation

**ABSTRACT:**

The process chain in optical measurement techniques can be subdivided into four main components: the camera system, the object range, the network design and the analysis system. The included influences (e.g. camera geometry, illumination, algorithms for image measurement) cause remaining deviations on the results due to insufficiently known effects on the photogrammetric system. This article will introduce a simulation technique based on Monte-Carlo-Methods to analyse effects of camera geometry, object space, signalisation and illumination. First two topics will be discussed based on simulation results. It allows a closer look at single system components, their uncertainty and randomly distribution simultaneously to the estimation of their influence on the photogrammetric system. The described Monte-Carlo-Simulation provides an economical process where the effects can be separated and modelled within an acceptable period of time and amount of work. It enables the determination of optimal system components (e.g. signalisation, illumination, camera geometry, analysis) and, in addition, the estimation of their influences on the process chain due to given (fixed) system components.

## 1. INTRODUCTION

The process chain in optical measurement techniques can be subdivided into four main components: the camera system (camera geometry, illumination), the object range (configuration, complexity, signalisation), the network design (configuration, scales, control elements) and the analysis system (algorithms for image measurement, functional model for camera geometry and bundle adjustment). Caused by this complex process chain photogrammetric results include remaining deviations due to insufficiently known effects.

Nowadays used digital high-resolution consumer cameras do not remain stable within an acceptable period of time, not within the period of image acquisition either. Therefore a new camera model was discussed and verified by Hastedt et al. (2002). An image-variant interior orientation is added to the functional model, which describes variation in principal distance and principal point. In order to compensate sensor based influences and remaining lens effects not considered within radial-symmetric lens distortion, a finite-elements sensor correction grid has been chosen. The mentioned camera model enables the use of instable digital high-resolution cameras for high precision purposes.

Choosing the right object range for calibration and verification purposes, the German Guideline VDI/VDE 2634, recommending a special configuration, gives particular support. Rautenberg & Wiggenhagen (2002) discussed the verification of different optical measuring systems based on this guideline. Hastedt et al. (2002) followed up this verification concept and demonstrated remaining length dependent deviations within the length measuring error.

In case of industrial measurement techniques retro-reflective material is used for signalisation combined with the use of ring-lights. Dold (1997) demonstrated the problem of this material. In particular the marginal reflection is affected and does not meet the required exact reflection. The choice of the material is an important component of the photogrammetric process, particularly regarding the subsequent measuring algorithm.

The optimization and specification of the network design has been discussed in several publications, e.g. Fraser (1984), Zinndorf (1986). Fraser (1984) explained the dependence on the Datum Problem (Zero-Order Design) and the Configuration Problem (First-Order Design). Regarding the optimization of the network design previous investigations and applied approaches have to be modified for recently used methods and new digital equipment and its advantages of flexible system components. One step towards this modification constitutes a simulation tool designed for special applications in crash-techniques, which has been developed by Raguse & Wiggenhagen (2003).

Having a closer look at the analysis system, two components are mainly influencing the systems result. First, belike one of the most important system parts, the algorithm (template matching, ellipse operator) measuring the centre of the imaged point mark has to be addressed. The importance of its influence is insufficiently known. Secondly the earlier described camera model.

In order to gain the single forces of the described components in an economical process where the effects can be separated and modelled within an acceptable period of time and amount of work, a simulation technique based on Monte-Carlo-Methods has been developed and will be introduced by this article. The simulation method allows a closer look at single system components, their uncertainty and randomly distribution simultaneously to the estimation of their influence on the photogrammetric system. The analysis of the simulation results of this report will focus on the influence of the camera parameters and geometry as well as on the influence of the object space, herein the systems exterior.

## 2. MONTE-CARLO-METHOD

The Monte-Carlo-Method (MCM) is a statistical simulation technique. Within the simulation process it generates a sample of non-interdependent variations of which the optimum will be chosen. The probability finding the absolute optimum increases with the number of simulation trials (Schmitt, 1977). Statistical simulation techniques are useful solving complicated linear systems. Furthermore the MCM can be used for solving problems, which focus on the evaluation of uncertainty and randomness of single system components, and additionally getting information about the whole systems behaviour, (Schwenke, 1999). Cox et al. (2001) divides the uncertainty evaluation process using MCM into two phases: Phase 1 includes as formulation phase the declaration of the probability density function (pdf) (1) of the input quantities (2).

$$g(X) = (g_1(X_1),...,g_n(X_n))^T \qquad (1)$$

$$X = (X_1,...,X_n)^T \qquad (2)$$

The pdf's, together with the measurement model constitute the inputs to the calculation phase (Phase 2) for the Monte-Carlo-Simulation process (Cox et al., 2001). Figure 1 shows the flow chart for a Monte-Carlo simulation process.
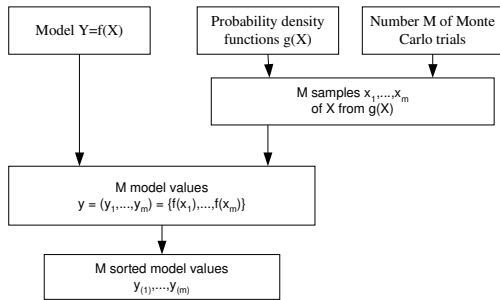


Figure 1. Flow chart of simulation process (Cox et al., 2001)

After specifying the functional model to be simulated, an appropriate probability density function g(X) needs to be selected. In this case of simulating photogrammetric bundles a univariate normal distribution, known as Gaussian distribution, has been chosen. Using numerical pseudo-random number generators uniform distributed numbers within an [0,1]-interval are the basis for randomly controlled simulation processes (Schmitt, 1977). Most programming languages support the generation of uniform distributed random numbers, algorithms like Hill-Wichmann or Kiss are applicable, too. The Box-Muller Algorithm (3) provides the generation of values from the standardized Gaussian distribution $N(0,1)$ (Cox et al., 2001). If $U_1$, $U_2$ are independent and identically continuous uniform distributed $U_{[0,1]}$ random values, the variables $X_1$ and $X_2$ defined by

$$X_1 = \sqrt{-2\log(U_1)}\cos(2\pi U_2)$$
$$X_2 = \sqrt{-2\log(U_1)}\sin(2\pi U_2) \qquad (3)$$

are then independent and identically univariate normal distributed $N_{[0,1]}$ values (Robert & Casella, 2002). All normal density curves (Gaussian distribution curve, Fig. 2) satisfy the following property. 68.3% of the observations fall within 1 standard deviation of the mean, 95.4% within 2 and 99.7% within 3 standard deviations of the mean for infinite random samples. Thus, for a normal distribution, almost all values lie within 3 standard deviations of the mean (Narasimhan, 1996). For finite-dimensional samples the normal distribution is replaced by the student's distribution (Graf et al. 1998).
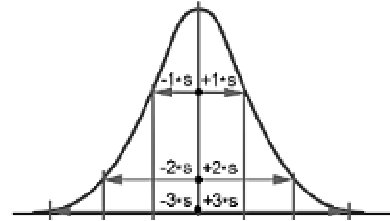


Figure. 2 Gaussian distribution curve

## 3. MODEL DEFINITION AND IMPLEMENTATION

The simulation process is based on existing and evaluated image bundles (*InputB*) that are made for verification purposes of high-resolution digital cameras. Therefore the whole simulation process is based on the standard observation equations. In case of evaluating the simulation process considering the described extended camera model, the standard observation equation is extended by image-variant parameters, which is explicitly exposed at Hastedt et al. (2002).

Due to many calculations caused by a high number of input values for one bundle adjustment, a step-by-step simulation is carried out. Caused by the definition of the C++ random number generator, all needed random numbers are first generated (Steps 1-2, Fig. 3). Dependent on the predefined number of Monte-Carlo trials (*S*), the process of data generation and calculation of the bundle adjustment will be executed *S* times. For each image *I* of one bundle the data generation will be executed as shown in Figure 3, Step 3.

First, camera parameters to be modified are randomly changed within their standard deviation arisen from the input bundle. In order to be able to analyse single system components and their influence within their standard deviation, the random modification of the camera parameters is selectable. One parameter of interior orientation will then be recalculated (4).

$$p_{(rm)} = p_{(iv)} + \left( nRNG_1 * s_p \right) \qquad (4)$$

with  $p_{(rm)}$ = randomly modified parameter

$p_{(iv)}$ = parameter's input value of *InputB*

$nRNG_1$ = normal distributed random value

$s_p$ = parameter's standard deviation of *InputB*

Afterwards the image coordinates need to be recalculated. Using the standard observation equation the image coordinates will be generated from predefined object space to image space

considering the generated camera parameters and randomly modified itself within their a priori standard deviation (4).
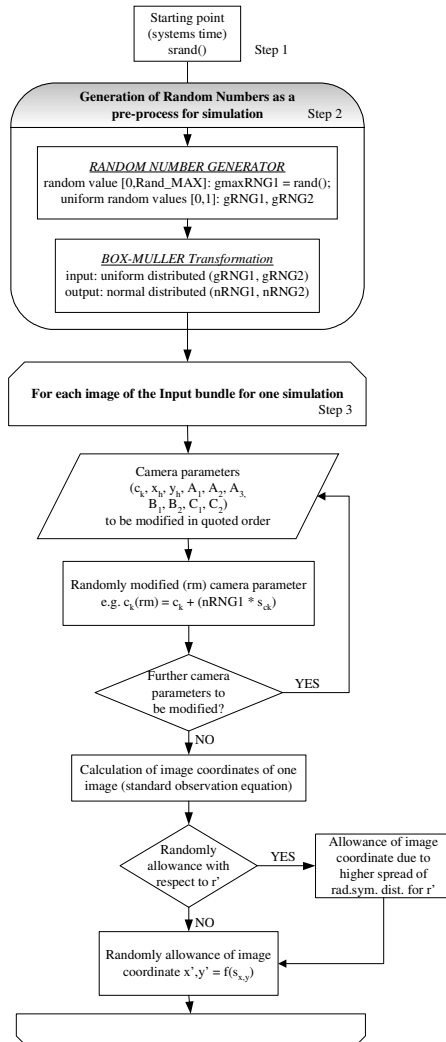


Figure 3. Flow chart of simulation data generation for one image *I* of one simulation process *S*

## Consideration of higher deviation of radial-symmetric distortion with respect to radial distance

The radial-symmetric lens distortion $A_1$, $A_2$, $A_3$ considers the highest influence of the distortion parameters. Due to its functional definition (5)

$$\Delta r' = r' \left( A_1 \cdot \left( r'^2 - r_0^2 \right) + A_2 \cdot \left( r'^4 - r_0^4 \right) + A_3 \cdot \left( r'^6 - r_0^6 \right) \right) \qquad (5)$$

with     $r'$  = radial distance
         $r_0$  = second zero-crossing
         $\Delta r'$  = radial-symmetric distortion

the standard deviation resp. its influence increases with the radial distance like graphically shown in Figure 4 for the following example (Table 1).

| Kodak DCS 645 M – 35mm lens | | | |
|---|---|---|---|
| Sensor format: 36.648 x 36.648 mm² | | | |
| ck | -35.6637 | sck | 0.0005 |
| xh | -0.0993 | sxh | 0.0007 |
| yh | 0.4083 | syh | 0.0007 |
| A1 | -9.01E-05 | sA1 | 1.56E-07 |
| A2 | 6.23E-08 | sA2 | 6.88E-10 |
| A3 | -1.48E-11 | sA3 | 9.20E-13 |
| B1 | 2.37E-06 | sB1 | 2.23E-07 |
| B2 | -1.46E-07 | sB2 | 2.21E-07 |
| C1 | 1.06E-04 | sC1 | 3.30E-06 |
| C2 | -1.04E-05 | sC2 | 3.17E-06 |

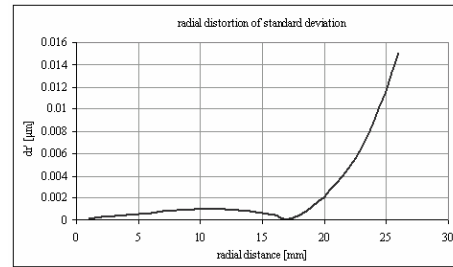Table 1. Example camera paramter



Figure 4. Standard deviation of radial-symmetric lens distortion

Applying this effect to the simulation process, an additive is calculated for the concerning image coordinate. In order to pursue the effect of the modified lens distortion with respect to the superior input bundle parameter, the additive's sign is generated of the difference of these two functional models. In the following this modification is called RADVAR-modification.

## 4. SIMULATION RESULTS AND ANALYSIS

The results and analyses are based on free-net bundle adjustments (free camera geometry), restrictively with three fixed scales placed to the coordinate systems axes. Because of the random generation of data sets, different blunder might appear due to an instable new data bundle. Modern bundle programs like BUNDY (own development of our institute), which is used for this simulation process, have integrated and non-changeable blunder detection algorithms. Strictly speaking the simulation results are based on different object geometry. The importance of this effect does mainly appear when scale points are eliminated within the calculation process, which causes different scales in object space. Concerning the following results and analyses these false-scaled bundle results are eliminated. In the following the expression input value defines the randomly modified values of the simulation process.

### 4.1 Camera geometry

**4.1.1   Input values**: With respect to the example of the Kodak DCS 645 M (Table 1) the normal distributed input values for principal distance and principal point result as shown in the diagrams (Fig. 5,6). The principal distance input values span from 36.66187mm to 36.66556mm. Regarding its standard deviation $s_{ck} = 0.0005$mm, 0.4% of all values (200 simulations * 60 images per bundle) lie outside the triple standard deviation, equally 0.4% of all values for the y-direction of the principal

point, which spans between –0.10194mm and –0.09664mm with reference to the standard deviation of $s_{xh,yh}$ = 0.0007mm. Due to a value range from 0.40561mm to 0.41106mm of the x-direction of the principal point, 0.2% of all random values lie outside 3σ. The values of the principal point resulting inside 3σ are framed in the space of the rectangle of Figure 6.
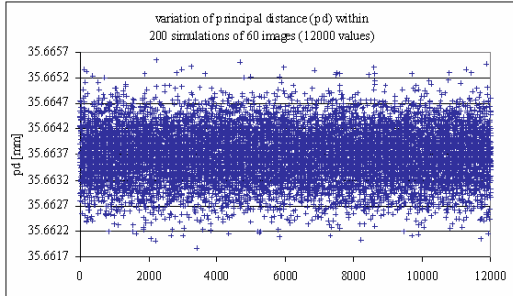


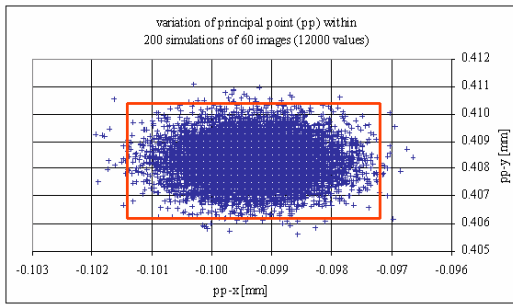Figure 5. Deviation of principal distance of simulation process



Figure 6. Variation of principal point of simulation process

The distortion curve of the input values of one simulation (hence 60 input values due to 60 images per bundle) results in Figure 7. The variation of distortion for large radial distances yield to ±70µm for one simulated bundle (Fig. 8). Due to the random modified parameters $A_1$, $A_2$, $A_3$ the distortion of maximum radial distance $r_{max}$ = 26mm varies up to 80 µm regarding all simulated values (Fig. 9). Comparatively the variation of dr' for a radial distance of 9mm yields to 6µm.

The consideration of this effect for the affected image coordinates seems to be significant. In particular regarding higher deviation of radial symmetric lens distortion with respect to the radial distance, the consideration of this variation is essential. With regard to the distortion of the InputB value for $dr'_{(rmax)}$ = -0.4115mm the deviation of ±40µm has significant influence on the image coordinates.

**4.1.2 Output values of bundle adjustments:** A closer look at the output values of the bundle adjustment with respect to the corresponding input values of the camera parameters demonstrates that the mean of the output values result in the InputB value for random modification (with reference to the example $x_h$ = -0.0993mm and Fig. 10). A generated random input value (4) with (6)

$$p_{(rm)} < p_{(iv)} \tag{6}$$

on the average results in a positive value for the difference of output and input value, vice versa to a negative value like illustrated in Figure 10. Ideally a straight line with a gradient of 1 would be obtained if no interacting effects would be considered within the functional model, herein the standard observation equations.
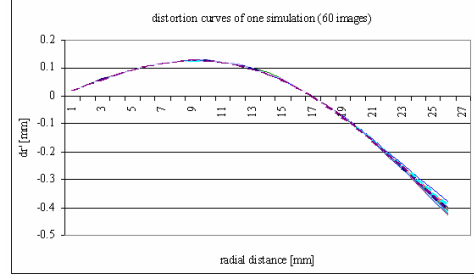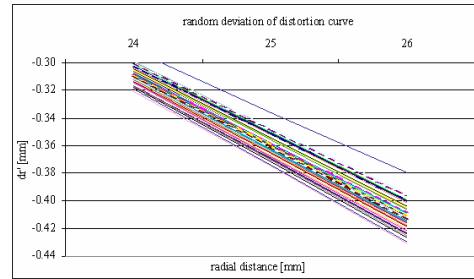


Figure 7. Lens distortion curve of one simulation



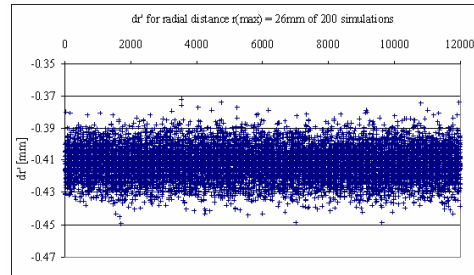Figure 8. Lens distortion for large radial distance



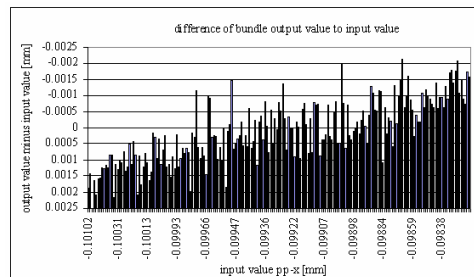Figure 9. Variation of dr' for $r_{max}$ of 200 simulations



Figure 10. Differences of output and input value

## 4.2 Object space

Due to simulated systems with non-real values the evaluation of the systems interior and exterior accuracy is based on the assumption that the simulated values vary within their standard deviation and therefore each random modified bundle represents a possible real bundle configuration. The systems exterior accuracy is represented by the error of length measurement (LME) of distances with respect to calibrated reference scales. The particular characteristics of the LME concerning the verification of optical 3D-measurement systems are described at VDI/VDE (2000). With respect to the example bundles, which are used for the simulation process and the analyses, the following LME are based on the reference testfield of our institute (Figure 11, interior cube).
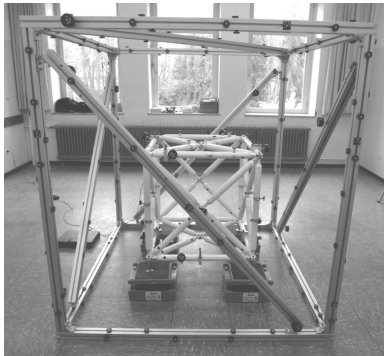


Figure 11. Photogrammetric testfield

The cube contains within a range of approx. 1m³ 14 reference targets, which are calibrated by a CMM, therefore 92 reference scales for analysing purposes. The accuracy of the reference scales represented by 3D-coordinates XYZ resulted in $RMS_{(XYZ)}[Ref] = 0.015mm$. With respect to the used camera system (Kodak DCS 645 M, example Table 1) and the network design an interior accuracy of one bundle can be expected as $RMS_{(XYZ)}[ObSp] = 0.040mm$ (7).

$$RMS_{(XYZ)} = \sqrt{[RMS(X)]^2 + [RMS(Y)]^2 + [RMS(Z)]^2} \qquad (7)$$

Because LME are influenced by both uncertainties, this results to an expected range of LME of ±60µm for 1σ, ±120µm for 2σ, ±180µm for 3σ.
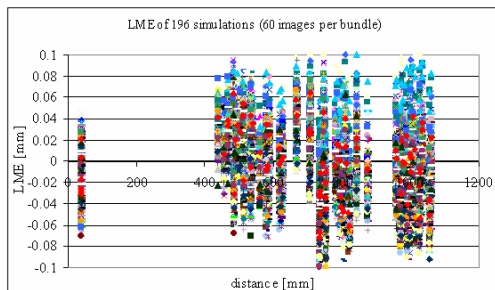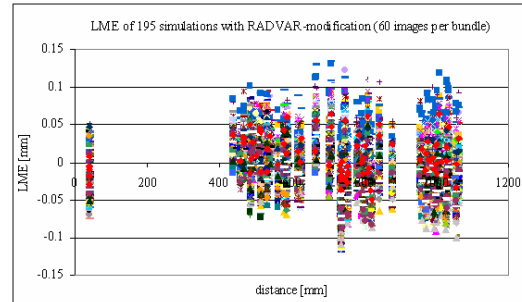


Figure 12. LME of 196 simulations



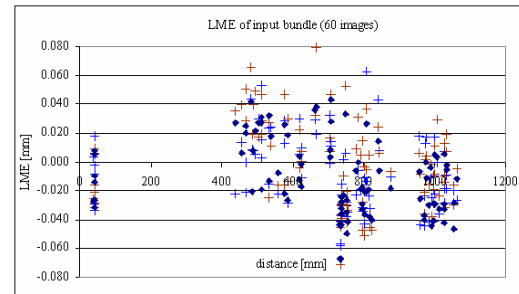Figure 13. LME for 195 simulations (RADVAR-modification)



Figure 14. LME of 2 results and overlaid InputB LME

Figure 12 shows the resulting LME for 196 successful random bundles of each 60 images. The remaining LME result within a range of ±100µm. Regarding the simulated bundles considering RADVAR-modification (Chapter 3) the LME result in a range of ±150 µm (Fig. 13). Due to a high number of LME values the differentiation and analysis within one comparative diagram cause difficulties. Therefore 2 results (crosses) are exemplarily illustrated in Figure 14. These two diagrams are overlaid by the LME of the input bundle (InputB) that are displayed with dark dots.

Summarizing the output values of the reference scales to a histogram, subdivided into 7 equal classes, the distribution results in an approximation of Gaussian distribution curves (Fig. 15).
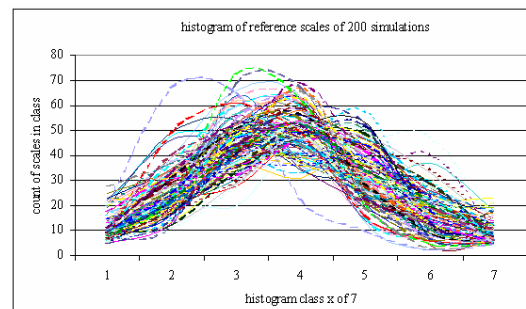


Figure 15. Histogram of reference scales

Due to the normal distributed input values this resulting distribution was expected. Hence the simulation process works properly for normal distributed random modified bundles. This effect is confirmed by resulting normal distributed output values for reference points with respect to the point of origin.

## 5. CONCLUSIONS

The simulation process introduced by this article allows the random modification of predefined input bundles. The generation of normal distributed values for the simulation process provides a defined number of photogrammetric bundles, which represent possible real bundle configurations. The results of the simulation process based on different input bundles show the successful implementation of the described simulation routine. The presented results are basis for further investigations, which are explicitly possible due to the simulation process. The Monte-Carlo-Method provides an economical process where the effects can be separated and modelled within an acceptable period of time an amount of work.

As a result of the successful simulation method for photogrammetric bundles, single effects of the different systems components can separately be changed. The advantage of this method is implied in the possibility to modify specific parameters. For instance, systematic effects can be applied and the influence can be modelled for analysing purposes. The separation of the effects included to the process chain of optical measurement techniques can therefore be controlled under laboratory investigations and be supported by practical experiments. The bundles are only influenced by one single effect whose impact can then be determined of the bundle adjustments results.

## 6. FURTHER INVESTIGATIONS

Due to finite-dimensional samples first the student's distribution will be applied to the simulation process. Likewise the distribution of image measurements need to be verified within practical trials and investigations of different illumination, signalization and image measurement techniques. The distribution of image coordinates is not dependent on the coordinate directions (x,y), but dependent on the imaging angle $\omega$ (Fig. 16).
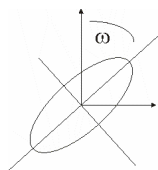


Figure 16. Imaging angle

The practical experiments and investigations will be linked to the simulation process in order to separate the influences.

Additionally the research will focus on the availability of high precise reference coordinates with regard to the verification concerning the German Guideline VDI/VDE 2634 for optical 3D measurement systems and their process chain component specifications.

## 7. REFERENCES

Cox, M. G., Dainton, M. P., Harris, P. M. (2001): Software Specifications for Uncertainty Calculation and Associated Statistical Analysis; NPL Report CMSC 10/01

Dold, J. (1997): Ein hybrides photogrammetrisches Industriemesssystem höchster Genauigkeit und seine Überprüfung; Schriftenreihe Universität der Bundeswehr München, Heft 54

Fraser, C.S. (1984): Network Design Considerations for Non-Topographic Photogrammetry; PE&RS Vol. 50, No. 8

Graf, Henning, Stange, Wilrich (1998): Formeln und Tabellen der angewandten mathematischen Statistik, Springer Verlag

Hastedt, H., Luhmann, Th., Tecklenburg, W. (2002): Image-variant interior orientation and sensor modelling of high-quality digital cameras; ISPRS Congress Com. V, Corfu

Narasimhan, B. (1996): The Normal Distribution; http://www-stat.stanford.edu/~naras/jsm/NormalDensity/NormalDensity.html

Raguse, K., Wiggenhagen, M. (2003): Beurteilung der Optischen Messkette durch Simulation der Aufnahmekonfiguration; Publikationen der DGPF, Band 12

Rautenberg, U., Wiggenhagen, M. (2002): Abnahme und Überwachung photogrammetrischer Messsysteme nach VDI 2634, Blatt 1; PFG, Nr. 2/2002, S. 117-124

Robert, C. P., Casella, G. (2002): Monte Carlo Statistical Methods; Springer-Verlag

Schmitt, G. (1977): Monte-Carlo-Design geodätischer Netze; AVN(84), 87-94, Heft 3/1977

Schwenke, H. (1999): Abschätzung von Meßunsicherheiten durch Simulation an Beispielen aus der Fertigungsmeßtechnik; PTB-Bericht: F-36

VDI/VDE 2634 (2001): Optical 3-D measuring systems – Imaging systems with point-by-point probing, VDI, Düsseldorf

Zinndorf, S. (1986): Optimierung der photogrammetrischen Aufnahmeanordnung; DGK, Reihe C, Heft Nr. 323